MDPI

Article

A Novel Strategy for Constructing Large-Scale Forest Scene: Integrating Forest Hierarchical Models and Tree Growth Models to Improve the Efficiency and Stability of Forest Polymorphism Simulation

Kexin Lei [1,2], Huaiqing Zhang [1,2,*], Hanqing Qiu [1,2], Tingdong Yang [1,2], Yang Liu [1,2], Jing Zhang [1,2], Xingtao Hu [1,2] and Zeyu Cui [1,2]

1 Institute of Forest Resource Information Techniques, Chinese Academy of Forestry, Beijing 100091, China; leikx@ifrit.ac.cn (K.L.); qiuhanqing123@ifrit.ac.cn (H.Q.); yangtd@ifrit.ac.cn (T.Y.); liuyang@ifrit.ac.cn (Y.L.); zhangjing@ifrit.ac.cn (J.Z.); 20010090319@gznu.edu.cn (X.H.); cuizeyu@ifrit.ac.cn (Z.C.)
2 Key Laboratory of Forestry Remote Sensing and Information System, The National Forestry and Grassland Administration, Beijing 100091, China
* Correspondence: zhang@ifrit.ac.cn; Tel.: +86-1-365-116-6672

Abstract: Modeling large-scale scenarios of diversity in real forests is a hot topic in forestry research. At present, there is a common problem of simple and poor model scalability in large-scale forest scenes. Forest growth is often carried out using a holistic scaling approach, which does not reflect the diversity of trees in nature. To solve this problem, we propose a method for constructing large-scale forest scenes based on forest hierarchical models, which can improve the dynamic visual effect of large-scale forest landscape polymorphism. In this study, we constructed tree hierarchical models of corresponding sizes using the detail attribute data of 29 subplots in the Shanxia Experimental Forest Farm in Jiangxi Province. The growth values of trees of different ages were calculated according to the hierarchical growth model of trees, and the growth dynamic simulation of large-scale forest scenes constructed by the integrated model and hierarchical model was carried out using three-dimensional visualization technology. The results indicated that the runtime frame rate of the scene constructed by the hierarchical model was 30.63 fps and the frame rate after growth was 29.68 fps, which met the operational requirements. Compared with the traditional integrated model, the fluctuation value of the frame rate of the hierarchical model was 0.036 less than that of the integrated model, and the scene ran stably. The positive feedback rate of personnel evaluation reached 95%. In this study, the main conclusion is that our proposed method achieves polymorphism in large-scale forest scene construction and ensures the stability of large-scale scene operation.

Keywords: large-scale forest scenes; stand structure; forest hierarchical model; dynamic visualization simulation of growth

1. Introduction

Forest ecosystems are highly complex and dynamic assemblages of biotic and abiotic webs that sustain human survival and development [1,2]; they play a crucial role in biodiversity conservation [3], wildlife habitat protection [4], forest products, and entertainment [5]. Visualization technology for tree growth utilizes three-dimensional simulation, enabling forest managers to intuitively perceive the individual tree growth states and forest resource distribution they are studying, which contributes to forest planning, forest decision-making, and forest resource management [5–8]. Therefore, large-scale three-dimensional forest simulation is vital for sustainable forest resource management. With the development of computer software, hardware, and graphic acceleration algorithms, many scholars at home and abroad have conducted relevant research on large-scale forest scene construction.

At present, the commonly used forest scene construction methods primarily include Polygon-Based Rendering [9,10], Image-Based Rendering [11,12], and Polygon and Image Hybrid Rendering [13]. The polygon-Based modeling method could fully exhibit individual tree polymorphisms. Therefore, heuristic multiresolution-based models [14], viewpoint multiresolution-based models [15], and other models were successively developed by grouping tree models, constructing the Level of Details (LOD) of different tree parts (trunk LOD, branch LOD, and leaf LOD) [16], and replacing tree geometric modeling that exceeded a certain distance by impostor texture replacement technology, which is considered an effective method for accelerating tree rendering [17]. Nowadays, some scholars use complex polygons to represent large objects and simple quadrilateral representations for small objects to accomplish large-scale scene rendering. Although geometric-based models have abundant structure details, the rendering speed is relatively slow and difficult in the application of large-scale forest scenes [18]. Due to the inability of geometric-based methods to meet people's needs, many scholars have focused on image-based methods. In contrast to simple geometric elements, images can present different aspects of complicated objects. Therefore, in the construction of large-scale forest scenes, image-based methods are the preferred selection technology. Some scholars have applied highly complex tree photos as a texture to a simple polygon to present the tree model information [19] and construct a forest landscape containing 100,000 trees using virtual reality modeling language (VRML) [20]. Volume texture was used to implement the individual tree visualization expression [21]. The trees generated offer multiple advantages; for example, they are more physically realistic and less time-consuming to create. However, they are essentially two-dimensional static images; therefore, they cannot fully exhibit the three-dimensional geometric structure of real trees, tree growth, and competition characteristics [22,23]. Although the speed satisfies the needs of large-scale rendering, the entire forest is relatively simple and cannot reflect the differences between individual trees. Geometric-based simplification methods can effectively simplify tree models, but the simplified models still contain a large number of triangular patches. Image-based simplification methods can greatly simplify tree models, but the close-up view is not ideal. Therefore, researchers have made attempts to mix geometric- and image-based methods in the simplification process of tree models to find a balance between magnitude and quality simplification [24]. SpeedTree software 9.0.0 (https://store.speedtree.com/, accessed on 20 May 2023) uses triangular patches to express the main branch structure of trees and a series of billboards to represent clusters of neighboring twigs and leaves. By introducing detailed textures, it generates a tree model that has a geometric structure and is highly physically realistic [13,25]. The tree models constructed with SpeedTree software are realistic, but large-scale forest scenes typically consist of tens of thousands of trees with variable shapes and morphologies. SpeedTree software requires numerous tree structural parameters to construct models with different shapes, which is time-consuming and laborious [26].

In addition, forest growth visualization simulation is an essential component of forest management and has great guiding significance for forestry production practice. Trees usually have diverse morphological characteristics [27,28]. In order to simulate tree growth status and spatial structure and predict the forest development succession more intuitively, vividly, and realistically, virtual forest construction methods based on stand growth laws have emerged [29]. Among them, some methods use individual tree growth models to calculate the growth parameters of forest morphological structures (diameter at breast height, tree height, and crown width) and use three-dimensional programming tools to accomplish stand growth visualization [30,31]. Some studies have developed distance-independent tree spatial growth models, which can better estimate stand development [32,33]. The distance-dependent models have the advantage that, in contrast to distance-independent models, their competition indices are optimized [34,35]. Some researchers have developed distance-dependent growth models from irregularly measured sample plot data; these allow model-based analyses of spatial problems such as systematic row thinning and different tree planting patterns [35–37]. By combining tree growth constraints, they also

use three-dimensional visualization and artificial intelligence (AI) algorithms to simulate the growth process of trees [7,38,39]. Although tree growth simulation has been achieved, many existing studies use discrete static simulation methods with overall scaling, but the polymorphism in the tree growth process cannot be depicted fully [40]. Existing studies on tree growth simulation generally follow the same pattern. In forestry, a tree growth model that conforms to the tree growth laws can be established on the basis of field-measured individual tree scale data. The growth parameters of various parts of individual trees can be calculated on the basis of the growth model, and three-dimensional visualization technology can be used to achieve dynamic visualization simulation of tree growth [41–43]. However, for large-scale forest scenes, the best way to model different characteristics of trees and dynamically simulate the polymorphism of the tree growth process problem remains unclear.

In summary, recent studies on forest scene dynamic visualization simulation mainly have focused on the construction and rendering optimization of small-scale stand scenes or middle-scale forest landscapes. However, fewer studies have been carried out on the construction of large-scale forest scenes combined with field-measured data, so large-scale forest scenes often exhibit the characteristics of a single form. Therefore, in order to address these issues, this study selected Shanxia Experimental Forest Farm as the study area to develop a large-scale forest scene with a tree hierarchical growth model based on data from 29 subplots. This study aimed to (1) develop a method for constructing a diverse large-scale forest scene using a tree hierarchical growth model; (2) conduct a comparative analysis on the construction of scenes with 100, 1000, 10,000, and 100,000 trees, respectively, to quantify the advantages of this research method compared with previous research methods; and (3) conduct a large-scale forest growth simulation using Unreal Engine 4 and tree hierarchical models and optimize the scene's rendering efficiency.

2. Materials and Methods

2.1. Study Areas

The study area was located in Shanxia Experimental Forest Farm (27°40′–27°45′ N, 114°35′–114°40′ E) in the southwest of Fenyi County, Xinyu City, Jiangxi Province, China (Figure 1). The forest farm has rich tree species resources, with 115,000 cubic meters of standing volume of living trees. The forest coverage is 95.6%. There are 115 precious broad-leaved tree species preserved, making it a relatively complete experimental forest in a subtropical region. The dominant tree species are *Cunninghamia lanceolata*, *Schima superba*, and *Machilus pauhoi*. It belongs to the subtropical monsoon climate with abundant rainfall and sunshine. The frost-free period is 270 days. It has abundant rainfall, with an annual precipitation of 1600 mm. The mean annual temperature is 15~17 °C. (Figure 1).

2.2. Data Collection

In May 2022, a sampling survey was conducted on 29 subplots in Shanyia Experimental Forest Farm, Fenyi County, and Jiangxi Province. Subplots are the fundamental management units within the forest farm and serve as the basic units for forest resource inventory, statistical calculations, and management. They are delineated according to ownership, land type, tree species, dominant tree species, and other factors. Considering the rich species diversity and high biodiversity of subplot 1, which makes it representative, all the trees in subplot 1 were measured. For other subplots with relatively homogeneous species composition, 2–3 sample plots with a size of 20 × 30, selected on the basis of the abundance of tree species and the good spatial structure of the forest stand, were used for the sampling survey. Tree species were identified by tree species experts. The relative coordinates (x, y, z) of the roots of each tree were measured using Topcon Total station made in Japan. The diameter at breast height (DBH) of each tree was measured using a DBH tape measure. A Leica D210 laser rangefinder made in Switzerland was used to measure the tree height (H) and the height under the living branches (UBH) of the trees. The crown width (CW) of the trees was measured using a tape measure. The crown height (CH) was

obtained by subtracting the height under the branches (UBH) from the tree height (H). The remaining 28 subplots were sampled and surveyed to obtain the main tree species, number of trees, average DBH, average H, average CW, average UBH, and average CH within the subplots. To build three-dimensional models of the trees, we used a Sony digital camera made in Japan to photograph the bark and leaf texture of the trees, shrubs, and herbs. The attribute data of 29 subplots are shown in Table 1.
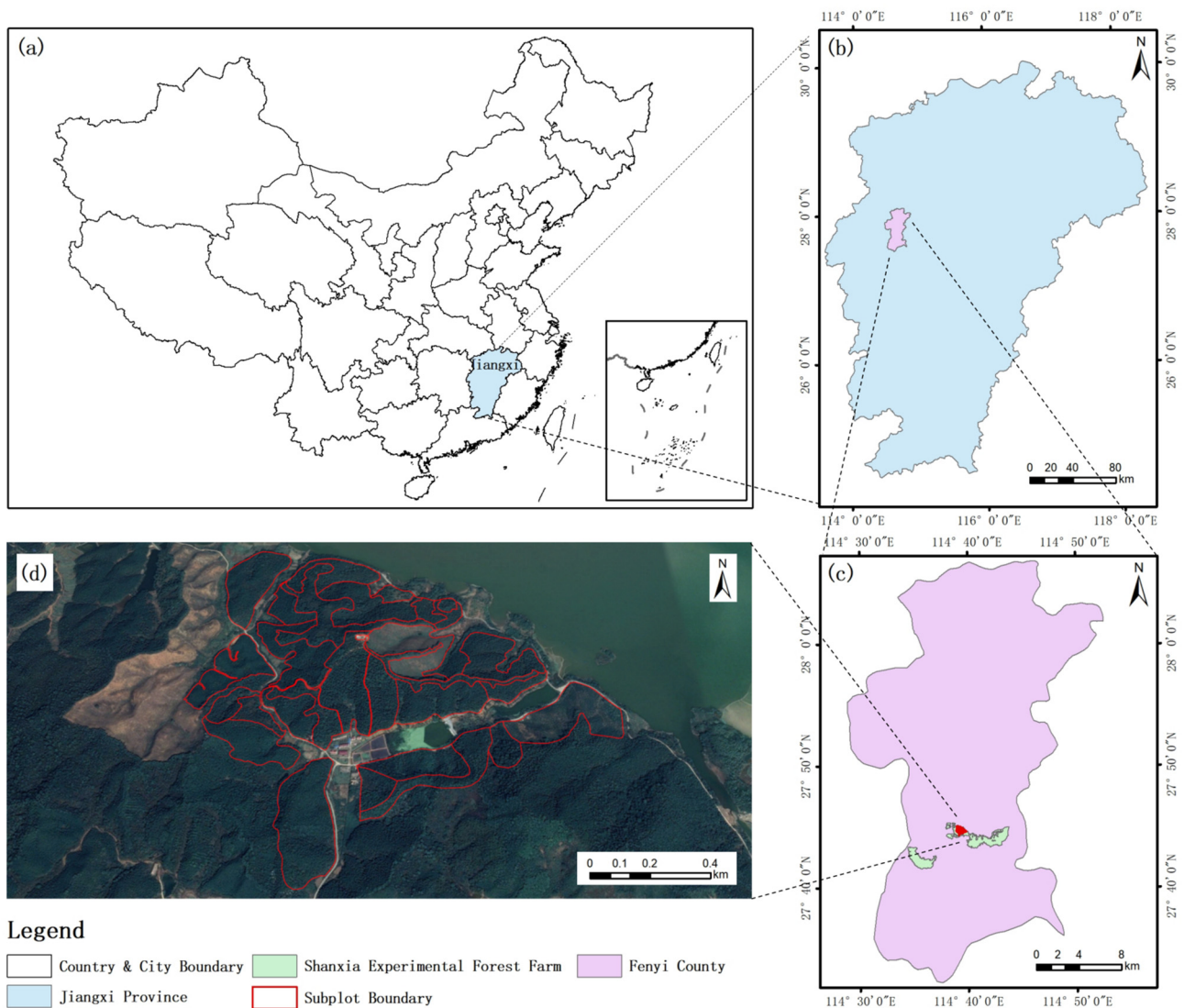
Figure 1. The location of the study area. (**a**) China's administrative boundary; (**b**) Jiangxi Province; (**c**) Fenyi County; (**d**) Shanxia Experimental Forest Farm. The red lines represent the subplot boundaries.

Table 1. Main forest stand attribute information of 29 subplots in Shanxia Experimental Forest Farm.

Subplot Number	Tree Species	Average DBH (cm)	Maximum Value	Minimum Value	Standard Deviation	Average H (m)	Maximum Value	Minimum Value	Standard Deviation	Average CW (m)	Number of Trees (Trees)	Canopy Density (%)	Stand Density (Trees/ha)	Area (ha)
1	*Cunninghamia lanceolata, Schima superba, Machilus pauhoi*	18.22	37.9	1.7	10.22	21.8	22.3	1.6	5.66	3.75	4092	70	54.25	5.03
2	*Cunninghamia lanceolata, Schima superba, Machilus pauhoi*	19.3	35.4	0.8	9.48	23.4	23.2	1.7	5.51	3.83	1896	70	52.79	2.39
3	*Cunninghamia lanceolata, Schima superba, Machilus pauhoi*	22.8	43.8	0.8	10.73	24.1	24.5	1.5	6.33	3.4	4042	70	71	3.80
4	*Cunninghamia lanceolata, Schima superba, Machilus pauhoi*	20.3	35.6	1.1	10.1	16.7	23.3	1.8	5.32	3.1	1156	70	65	1.19
5	*Cunninghamia lanceolata*	24.5	52.9	0.8	11.06	18.5	26	1.5	6.75	3.33	3729	70	53	4.69
6	*Schima superba*	31.5	35.5	1	10.21	31.9	22.8	1.9	5.62	8.5	978	80	35	1.86
7	*Cunninghamia lanceolata*	6.2	42.3	1	12.64	3.1	23.6	1.8	6.74	4.2	4161	70	50	5.55
8	*Cunninghamia lanceolata*	16.4	39	0.6	10.82	17.5	25.7	1.6	7.18	2.6	929	70	78	0.79
9	*Schima superba, Sassafras tzumu, Cinnamomum camphora*	21.2	39.3	2.3	9.67	20.2	22	3.1	4.6	7.1	199	75	29	0.46

Table 1. *Cont.*

Subplot Number	Tree Species	Average DBH (cm)	Maximum Value	Minimum Value	Standard Deviation	Average H (m)	Maximum Value	Minimum Value	Standard Deviation	Average CW (m)	Number of Trees (Trees)	Canopy Density (%)	Stand Density (Trees/ha)	Area (ha)
10	*Schima superba, Sassafras tzumu*	24.5	46.5	0.6	10.95	21.5	24.5	1.6	6.73	6.74	685	70	43	1.06
11	*Cunninghamia lanceolata*	22.5	36.9	0.6	10.36	22	25.8	1.8	6.42	3.33	7238	75	78	6.19
12	*Cunninghamia lanceolata, Schima superba*	20.3	45.1	1.1	11.66	18.1	24.4	1.9	7.48	4.65	4458	75	77	3.86
13	*Schima superba, Castanopsis sclerophylla, Cinnamomum camphora, Sassafras tzumu*	26.2	35.4	2.6	8.39	14.6	21.9	2.9	4.4	5.4	481	60	33	0.97
14	*Cunninghamia lanceolata*	22.8	46.5	0.3	11.39	18.6	24.1	1.8	6.18	3.65	2029	70	74	1.83
15	*Pinus massoniana, Cunninghamia lanceolata, Vernicia fordii*	21.5	36.7	1.3	7.36	15.9	23	3.7	3.68	5.31	7674	85	85	6.02
16	*Cunninghamia lanceolata*	24.1	39.6	2.2	9.43	20.2	22.8	4	4.8	4.05	5811	70	78	4.97
17	*Schima superba, Vernicia fordii*	29.4	42.4	1	11.02	19.5	21.5	1.5	4.85	8.5	3896	70	40	6.49
18	*Cunninghamia lanceolata*	13.8	42.1	1.2	11.52	12.2	24.3	2.2	6.84	2.54	11629	95	162	4.79
19	*Cunninghamia lanceolata*	27.5	46.1	3.3	9.88	21.1	23.1	0.7	5.11	3.62	1656	70	82	1.35

Table 1. *Cont.*

Subplot Number	Tree Species	Average DBH (cm)	Maximum Value	Minimum Value	Standard Devia-tion	Average H (m)	Maximum Value	Minimum Value	Standard Devia-tion	Average CW (m)	Number of Trees (Trees)	Canopy Density (%)	Stand Density (Trees/ha)	Area (ha)
20	*Castanea mollissima, Paulownia fortunei, Cunninghamia lanceolata*	17.6	45	2	11.29	12.7	25.4	2.7	6.23	7.21	921	70	48	1.28
21	*Michelia platypetala*	21.2	41.2	4.9	4.92	16.5	19.6	2.1	2.08	4.05	2725	60	52	3.49
22	*Liriodendron tulipifera*	17.9	38.4	4.5	8.63	17.8	23.1	1.5	5.02	4.69	1411	75	71	1.32
23	*Vernicia fordii, Machilus pauhoi*	22.3	37.2	2	9.11	13.7	22.6	3.7	4.44	7.65	1542	75	29	3.55
24	*Cunninghamia lanceolata, Schima superba, Paulownia fortunei*	19.4	37.1	4.5	4.55	15.6	24.3	2.9	2.98	5.78	2419	85	95	1.70
25	*Cunninghamia lanceolata, Schima superba, Machilus pauhoi*	19.22	38.1	1.5	7.62	22.2	20.8	2.7	3.49	4.15	1547	75	52	1.98
26	*Cunninghamia lanceolata*	27.4	39.1	2.7	7.12	18.8	17.7	3.2	3.34	3.24	2213	75	71	2.08
27	*Cunninghamia lanceolata*	14.7	33.5	0.8	8.83	12.8	17.3	1.1	3.96	1.81	15539	90	158	6.56
28	*Schima superba, Cinnamomum camphora, Vernicia fordii*	15.2	38.3	1.3	7.58	12.1	22.7	1.4	3.57	2.24	6764	85	121	3.73
29	*Myrica rubra*	9.8	33.2	1.6	7.36	4.2	15.4	0.9	1.98	4.55	6344	65	60	7.05

2.3. Data Analysis

2.3.1. Construction and Decomposition of Three-Dimensional Tree Model

At present, there are many tools for tree modeling [44–46]. We used SpeedTree three-dimensional modeling software, combined with the forest morphological and structural parameters of the main common tree species collected at the Shanxia Forest Farm, including H, DBH, UBH, CW, CH, azimuth angle, and other parameters, as well as the morphology and texture photos of the trees. We selected the morphological and structural parameters of the trees with a good growth status and morphological structure for various tree species. We added the trunk, branches, twigs, and leaves to the SpeedTree software; adjusted parameters such as trunk curvature and branch angle; and pasted the texture of the bark and leaves. Eventually, we constructed initial three-dimensional models for 32 tree species, including *Cunninghamia lanceolata*, *Schima superba*, and *Machilus pauhoi*. The model was constructed using backward elimination technology, which only displays faces facing the screen, improving the rendering efficiency of the three-dimensional model of the forest canopy. Finally, 32 three-dimensional models of forest trees were constructed in order to better reflect the different morphological and structural characteristics of trees in forest scenes and ensure that the changes in the various directions of the trees during the growth process conformed to the law of the forest. In this study, on the basis of the morphological characteristics of forest trees, we decomposed the three-dimensional model of forest trees into two models: trunk and crown. Each model was considered an independent unit, reflecting the growth and variation trends of H, DBH, CH, UBH, and CW. Taking *Cunninghamia lanceolata* as an example, the three-dimensional model and decomposition model of *Cunninghamia lanceolata* are shown in Figure 2.
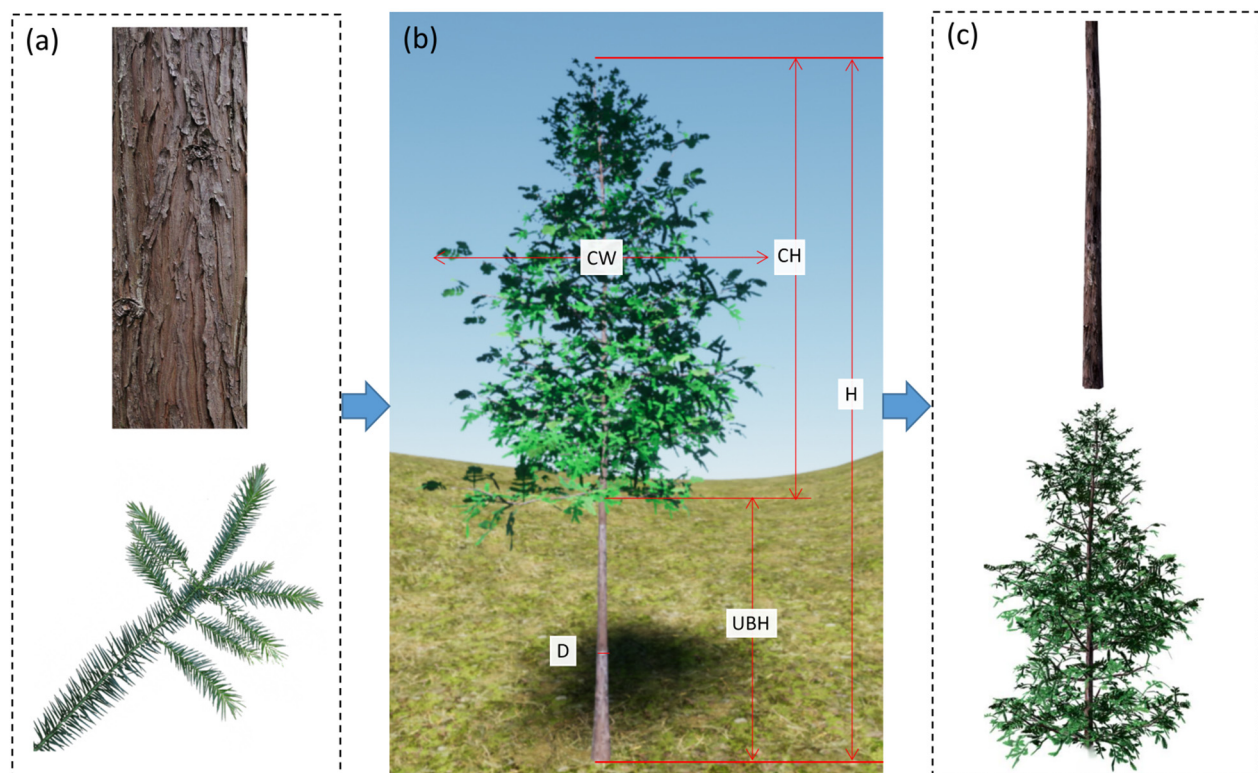

Figure 2. (**a**) Representation of the texture of the bark and leaves of *Cunninghamia lanceolata* trees. (**b**) The initial three-dimensional model of *Cunninghamia lanceolata* created using (**a**,**b**) and real measurement data. (**c**) Representation of the hierarchical model of *Cunninghamia lanceolata*.

2.3.2. Tree Hierarchical Growth Model

The forest growth model is a mathematical model that describes the growth process of trees. It is generally used to describe the relationship between tree volume and growth age [47]. In order to simulate the polymorphism of forest trees more realistically during the growth process, we used DBH, H, UBH, CH, and CW as the main parameters of forest tree morphology and structure in this study. The DBH growth model and the UBH growth model were used for the tree trunk, while the CW growth model and the CH growth model were used for the tree crown. According to the results of on-site inspections on Shanxia Forest Farm, 12 main distributed tree species were selected for growth simulation. We calculated the values of the tree DBH, H, CW, UBH, and CH after years of growth on the basis of the current age of the trees using other studies and the growth models provided by local forest farms for each tree species. Taking *Cunninghamia lanceolata* as an example, the growth models are shown in Table 2.

Table 2. Hierarchical growth model of *Cunninghamia lanceolata*.

ID	Model Name	Growth Model	Description	References
1	DBH growth model	$D = 21.7106 * \left(1 - e^{-0.0538*age}\right)^{0.7626}$	*D* represents diameter at breast height of tree, age represents time of growth	[48]
2	H growth model	$H = 20.3793 * \left(1 - e^{-0.0684*age}\right)^{1.1943}$	*H* represents height of tree, age represents time of growth	[48]
3	CW growth model	$CW = 0.660 + 0.037 \times age + 0.160 \times Ph$	*CW* represents crown width of tree, *Ph* represents horizontal structural parameters (minimum distance affected by adjacent trees)	[49]
4	CH growth model	$CH = -3.036 + 0.469 \times age + 2.690 \times Pv$	*CH* represents crown height of tree, *Pv* represents vertical spatial structural parameters (the average relative height of adjusted trees)	[49]
5	UBH growth model	$UBH = -3.020 + 0.409 \times age + 2.601 \times Pv$	*UBH* represents height under the branches of tree, *Pv* represents vertical spatial structural parameters (the average relative height of adjacent trees)	[49]

2.3.3. Visualization Simulation of Large-Scale Forest Scene Growth Dynamics Based on Forest Hierarchical Model

In traditional large-scale forest scenes, trees are often scaled proportionally using an integrated model. Integrated models consider the trees as a whole and calculate the actual values of UBH, CW, and CW on the basis of the growth models of H and DBH. This is unreasonable. The hierarchical model divides the model into the trunk and the crown, which can be calculated according to the growth models of different parts, making the large-scale forest landscape more diverse.

Using Unreal Engine 4 (UE4, https://www.unrealengine.com/zh-CN, accessed on 25 May 2023), which is an efficient and versatile game development engine launched by Epic Games, we can directly preview the three-dimensional simulation development effect [44]. We connected to the MySQL database with UE4 and read the stand data table. The three-dimensional model of a tree is divided into two parts: the trunk and the crown. The original point of the coordinates of the trunk and the crown of the tree hierarchical model was assumed to be at the bottom. The initial DBH of the trees in the forest is $D_{initial}$, the height of the trees is $H_{initial}$, the crown width is $CW_{initial}$, the height under branches is $UBH_{initial}$, and the crown height is $CH_{current}$. The current DBH of the trees in the scene is $D_{current}$, the height of the trees is $H_{current}$, the crown width is $CW_{current}$, the height under branches is $UBH_{current}$, and the crown height is $CH_{current}$. The DBH of the trees after growth is D_{grow}, the height of the trees is H_{grow}, the crown width is CW_{grow}, the height under branches is UBH_{grow}, and the crown height is CH_{grow}.

According to the timeline animation event, the forest growth model library (which used the growth model that conformed to the growth of the dominant species provided by the forest farm locally), and the blueprint function script (which is a visual script that provides an intuitive, node-based interface and realizes code programming by dragging and dropping nodes), a set of forest growth blueprint function scripts was built. The scaling coefficient of the initial scene tree was calculated through a function script, and the scaling coefficient after tree growth was calculated according to the annual growth of each part of the tree in real time.

Using LOD technology, the forest hierarchical model and field measurement data were used to construct an initial scene of a real Shanxia Experimental Forest Farm. When the viewpoint is far away, the trees are displayed in the form of billboards. As the viewpoint approaches, a mixture of graphics and images is gradually adopted. When observing the tree morphology at close range, full three-dimensional graphics are used to display the details of the trees. The dynamic visualization simulation process of large-scale forest scene growth is shown in Figure 3.
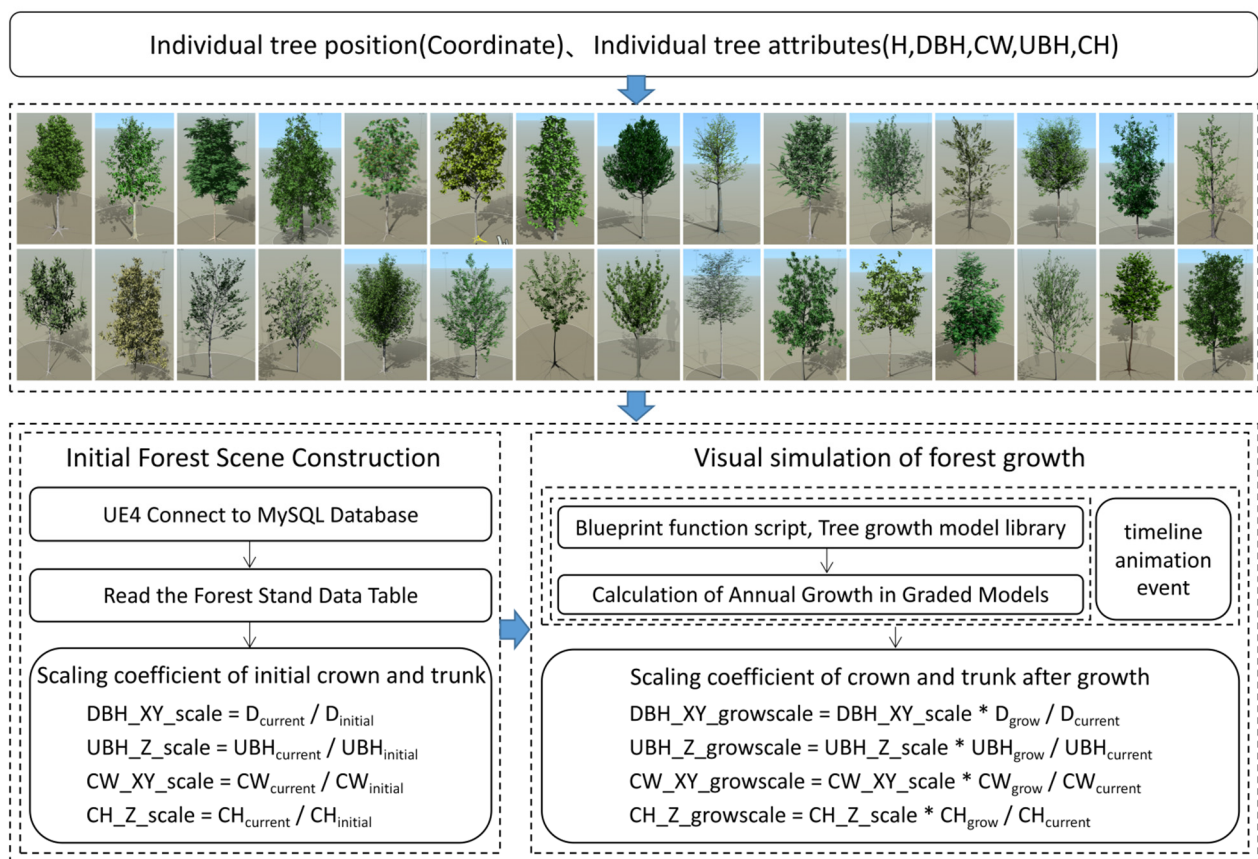

Figure 3. The dynamic visualization simulation process of large-scale forest scene growth.

2.3.4. Evaluation Indicators for Large-Scale Forest Scene Construction
Frame Rate

We compared the performance of scenes using two indicators: frame rate and frame rate fluctuation value (F).

The number of frames refreshed per second was measured in frames per second (fps). Frame rate is an important evaluation indicator for rendering rate in virtual scenes, requiring a frame rate of no less than 30 fps. The higher the frame rate, the smoother the

visual display, and the smoother the screen image. Its size determines the smoothness that the user feels when rendering. The frame rate calculation formula is shown in (1).

$$Frame\ rate = frameNum/elapsedTime \tag{1}$$

Frame rate fluctuation value can be obtained by calculating the standard deviation of the frame rates. When calculating the frame rate variability, it is necessary to record the frame rate of each frame during a certain period of time and then calculate the standard deviation of these frame rates. The smaller the frame rate fluctuation value, the more stable the scene runs. The frame rate fluctuation value calculation formula is shown in (2).

$$F = \sqrt{\frac{\sum_{i=1}^{n}\left(Frame\ rate_i - \overline{\sum_{i=1}^{n}Frame\ rate_i}\right)^2}{n}} \tag{2}$$

where *Frame rate$_i$* represents the frame rate of the ith frame, and *F* represents the frame rate fluctuation value.

Forest form Evaluation Method

The evaluation of scene quality involves a subjective judgment process. In this study, we adopted a manual evaluation method. We recruited 20 graduate students, including 9 males and 11 females, to participate in the assessment. Males accounted for 45% of the selected sample, while females accounted for 55%. We invited them to conduct experiential simulations of the large-scale forest scene that we constructed and asked them to rate the similarity between the real scenes and the virtual scenes. Accoridng to the recorded scoring results, we quantitatively analyzed the authenticity and reliability of our constructed scene.

3. Results

3.1. Forest Hierarchical Model

Taking 4092 trees in subplot 1 as an example, Table 3 shows the distribution of tree numbers within the ranges of 0–15 cm, 15–30 cm, 30–45 cm, 45–60 cm, 60–75 cm, 75–90 cm, and >90 cm for constructing large-scale forest scenes using hierarchical and integrated models. It can be seen that the hierarchical model used each attribute factor of the tree with a wide distribution of values, such as H, CH, DBH, CW, and UBH, solving the problem of traditional large-scale forests exhibiting a uniform appearance for thousands of trees. The integrated model used two parameters, H and DBH, which can only reflect the H and DBH of each tree. The CW, CH, and UBH increased with the increase in DBH, and the forest form was single.

Table 3. The distribution of tree attributes within the ranges of 0–15 cm, 15–30 cm, 30–45 cm, 45–60 cm, 60–75 cm, 75–90 cm, and >90 cm in the hierarchical model and integrated model.

Tree Attributes	0–15 (cm)		15–30 (cm)		30–45 (cm)		45–60 (cm)		60–75 (cm)		75–90 (cm)		>90 (cm)	
	Hierarchical Model	Integrated Model	Hierarchical Model	Integrated Model	Hierarchical Model	Integrated Model	Hierarchical Model	Integrated Model	Hierarchical Model	Integrated Model	Hierarchical Model	Integrated Model	Hierarchical Model	Integrated Model
DBH (trees)	1907	1907	1620	1620	539	539	26	26	0		0	0	0	0
CW (trees)	112	-	1276	-	1773	-	635	-	208		67	-	21	-
H (trees)	2	2	4	4	49	49	207	207	389		487	487	2954	2954
CH (trees)	35	-	242	-	477	-	611	-	605		530	-	1592	-
UBH (trees)	329	-	1263	-	913	-	534	-	393		318	-	342	-

We conducted a visual simulation of the hierarchical model and the integrated model before and after growth, respectively. The morphological changes in hierarchical and integrated models currently and after 10 and 20 years of growth are shown in Figure 4. The results showed that as the trees grow, the changes in tree DBH and UBH can be clearly seen, as shown in Figure 4a–c. However, Figure 4e,f only shows a proportional increase

in tree H and CW, and the DBH and CW are scaled according to the same scaling factor, resulting in morphological structure parameters of the forest that are inconsistent with the actual growth pattern.

Figure 4. The morphological changes in hierarchical and integrated models after 10 and 20 years of growth. (**a**–**c**) Morphological changes of hierarchical model currently and after 10 and 20 years of growth. (**d**–**f**) Morphological changes of integrated model currently and after 10 and 20 years of growth.

3.2. Visual Simulation Result Evaluation

Taking the data of the tree information in the Shanxia Forest Farm as an example, a hierarchical model and an integrated model were used to simulate and analyze the spatial distribution of forests in different growth stages. The method of the hierarchical model was to calculate the UBH and CW under the branches using the growth model of UBH and the growth model of CW. The method of the integrated model was to calculate the corresponding UBH and CW proportionally on the basis of the H growth model and the DBH growth model. Due to the long growth cycle of trees, we compared the growth simulation results with sample plots with similar site conditions and tree ages in terms of the branch height and crown width in this paper. The simulation results and actual measurement results of UBH at different ages using the two methods are shown in Table 4, and the simulation results of CW are shown in Table 5. At 40 and 50 years, the average predicted values and errors of the UBH and CW of the hierarchical model were smaller than those of the integrated model. The standard deviation of the predicted values of the hierarchical model was smaller than that of the integrated model, indicating that the values calculated by our method were closer to the actual values.

Table 4. The actual value and growth value of the UBH in the hierarchical model and the integrated model.

Origins			40 Years Old				50 Years Old				
Age (Year)	UBH (m)	Measurements	Hierarchical Model		Integrated Model		Measurements	Hierarchical Model		Integrated Model	
			Forecasts	Error	Forecasts	Error		Forecasts	Error	Forecasts	Error
15	1.6	7.8	8.3	0.5	8.7	0.9	9.4	9.6	0.2	9.8	0.4
15	1.4	7.6	8.8	0.8	6.5	1.1	9.2	10.4	1.2	10.5	1.3
20	2.9	8.2	9	0.8	7.4	0.8	10.1	10.5	0.4	9.4	0.7
20	3.1	8.4	8.7	0.3	8.9	0.5	10.3	11.3	1.1	11.7	1.4
25	4.9	8.1	8.5	0.4	8.7	0.6	9.8	10.1	0.3	9.2	0.6
25	5.8	9.3	10	0.7	8.5	0.8	11.5	11.7	0.2	11	0.5
30	7.1	9	7.3	1.7	11.1	2.1	10.6	11.2	0.6	9.7	0.9
Mean value	3.83	8.34	8.66	0.74	8.54	0.97	10.13	10.69	0.57	10.19	0.83
Standard deviation	5.29	1.51	1.98	1.14	3.49	1.31	1.91	1.82	1.03	2.24	0.96

Table 5. The actual value and growth value of the CW in the hierarchical model and the integrated model.

Origins			40 Years Old				50 Years Old				
Age (Year)	CW (m)	Measurements	Hierarchical Model		Integrated Model		Measurements	Hierarchical Model		Integrated Model	
			Forecasts	Error	Forecasts	Error		Forecasts	Error	Forecasts	Error
15	2.9	6.2	7.1	0.9	7.6	1.4	8.1	8.8	0.7	9	0.9
15	2.7	5.9	7.2	1.3	7.4	1.5	7.9	8.2	0.3	7.3	0.6
20	3.3	6.3	7.4	1.1	7.4	1.1	7.8	8.4	0.6	7	0.8
20	3.4	6.7	7.4	0.7	7.6	0.9	7.6	8.8	1.2	9.1	1.5
25	4.1	5.8	6.4	0.6	7	1.2	8.2	9	0.8	9.4	1.2
25	4.3	6.1	6.9	0.8	7.7	1.6	8.5	9.4	0.9	7.2	1.3
30	5.2	6.9	7.4	0.5	6.1	0.8	8.9	9.3	0.4	8	0.9
Mean value	3.7	6.27	7.11	0.84	7.26	1.21	8.14	8.84	0.70	8.14	1.03
Standard deviation	2.16	0.99	0.9	0.69	1.37	0.74	1.09	1.08	0.75	2.48	0.77

We invited 20 students to compare and rate the constructed large-scale forest scene with the real DigitalOrthophoto Map (DOM) image of the Shanxia Experimental Forest Farm (Figure 5). The evaluation results were mainly decided from four forest scene indicators: scene similarity, scene immersion (whether one feels the authenticity of the environment and the sense of immersive participation), scene fluency, and forest polymorphism. The results of four forest scene indicators are shown in Table 6. In Figure 5a,e, it can be seen that the distribution of the 29 subplots was basically consistent with the DOM. Among them, 19 people thought that the scene authenticity was very high, and 1 person thought that the scene authenticity was general, with a satisfaction evaluation rate of 95%. Twenty

people thought that the scene immersion was good, with a satisfaction evaluation rate of 100%. Eighteen people thought that the scene fluency is good, and two people thought that it is general, with a satisfaction evaluation rate of 90%. In addition, 19 people thought that the scene reflected the polymorphism of the forest very well, while one person thought that the scene did not reflect the polymorphism of the forest very well, with a satisfaction evaluation rate of 95%.
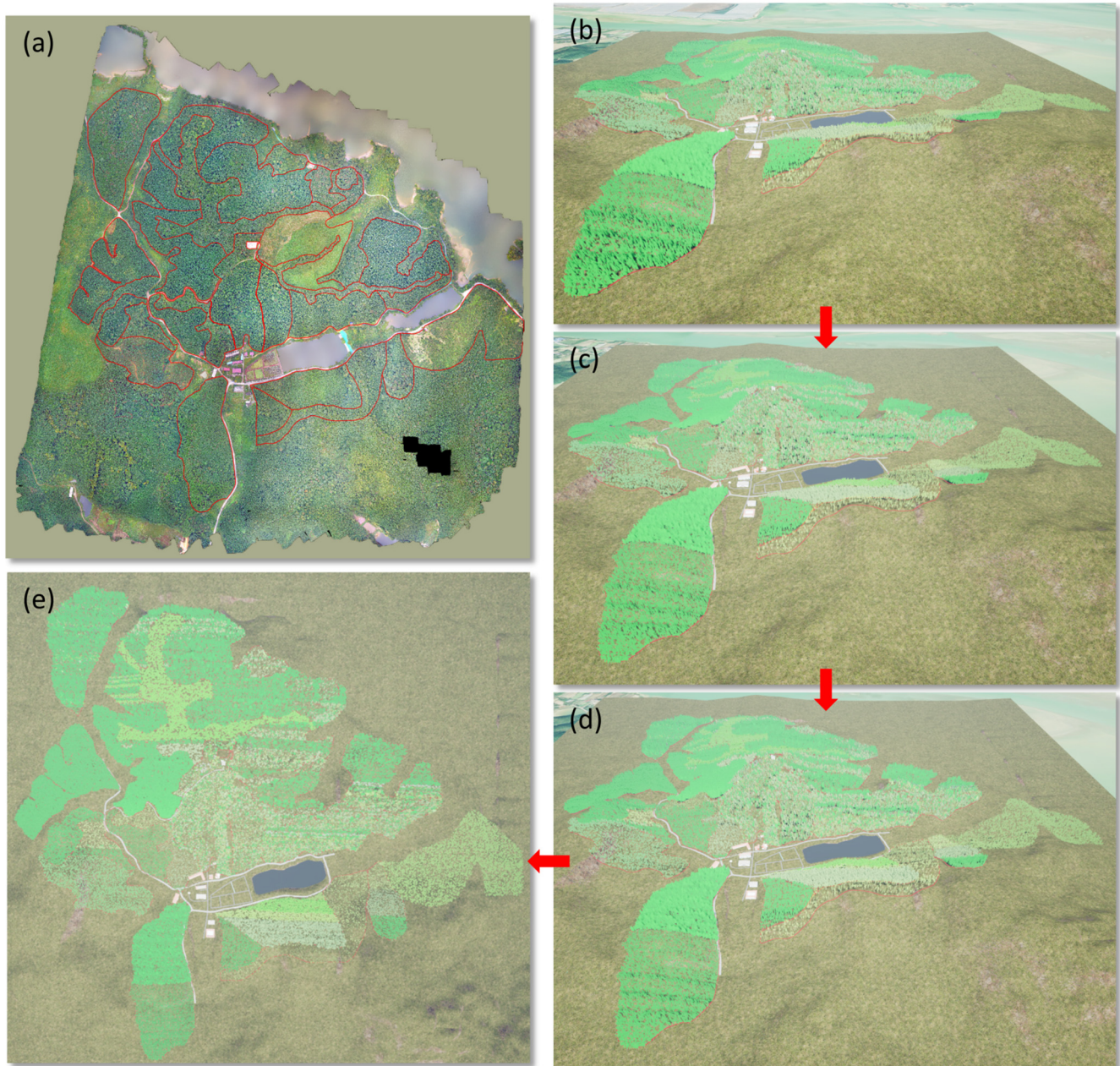

Figure 5. Comparison between real images and forest scene simulations. (**a**) Representation of the DOM of Shanxia Experimental Forest Farm. (**b**–**e**) Representation of the visual simulation scenes of Shanxia Experimental Forest Farm. Red arrow indicates the forest scene from different angles of the camera.

Table 6. Evaluation of forest scene indicators.

Evaluation Index	Good	General	Poor
Scene similarity	19	1	0
Scene immersion	20	0	0
Scene fluency	18	2	0
Forest polymorphism	19	1	0

The results showed that (1) the constructed large-scale forest scene had high similarity and strong immersion with the real forest farm, and the satisfaction evaluation rate was 95%. Therefore, the construction of large-scale forest scenes using the forest hierarchical model can more vividly and intuitively express and analyze the forest. (2) The construction of large-scale forest scenes using the forest hierarchical model has good running fluency, and trees of different shapes and sizes improve the visual effect of traditional large-scale forest scenes.

3.3. Visualization Simulation of Large-Scale Forest Scene Growth Dynamics

The three-dimensional models constructed with 32 kinds of trees using by SpeedTree software were added to the three-dimensional scene as a class, and we read the coordinates in the stands data table through the inaccurate transform longitude latitude height to the unreal node under the CesiumGeoreference reference in the Unreal Engine 4 rendering engine [50]. The hierarchical growth model and traditional integrated model scaling method were used to draw forest scenes of 10 trees, 100 trees, 1000 trees, 10,000 trees, and 100,000 trees in the Shanxia Forest Farm. The horizontal changes of the forest scene from different height perspectives are shown in Figure 6. The spatial structure characteristics of the forest, such as the diversity of tree species, the size difference, the spatial distribution pattern of trees, and the compression between tree crowns, can be clearly seen. As shown in Figure 6g,h, we could directly observe the uneven distribution or poor growth of trees caused by competition.

The average frame rate and system average frame rate fluctuations before and after growth are shown in Table 7. It can be seen that both two methods achieved a frame rate of over 50 fps when drawing 10, 100, and 1000 trees in small-scale forest scenes. When drawing large-scale forest scenes, such as scenes with 10,000 and 100,000 trees, the method proposed in this study based on a hierarchical model achieved a minimum frame rate of 30.63 fps for forest scenes, which meets people's needs for scene rendering. The minimum frame rate of the integrated model was 30.74 fps, which was 0.11 fps higher than the frame rate of the proposed hierarchical model. The frame rate of the integrated model after growth was 29.68 fps, which was 0.96 fps higher than the frame rate of the hierarchical model proposed in this study. In general, the integrated model ran at a high frame rate, but the constructed forest scene had the problem of "a thousand trees are all similar".

Table 7. The average frame rate and system average frame rate fluctuations before and after growth using hierarchical and integrated model methods.

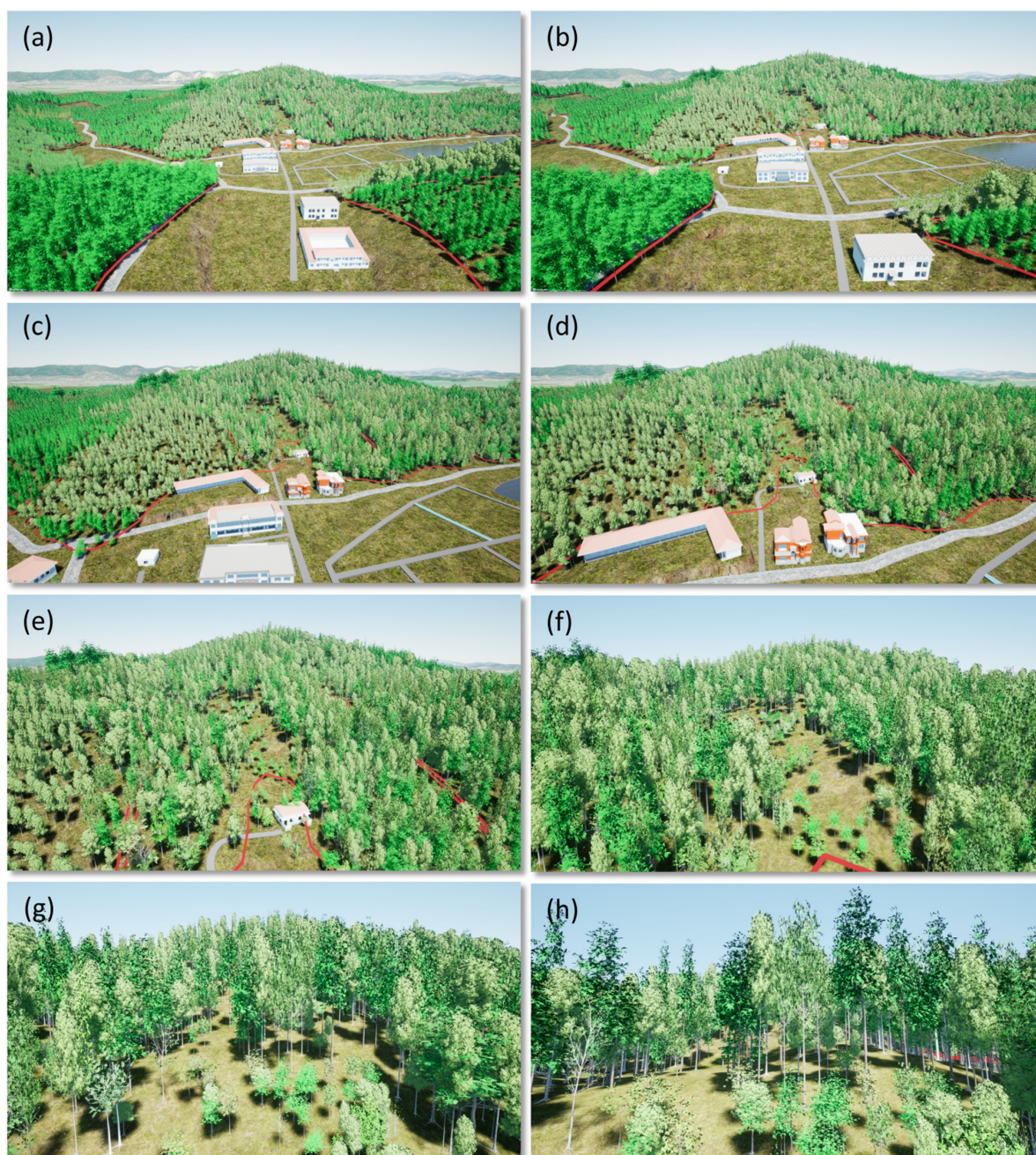| Number of Trees	Before Growth				After Growth			
	Hierarchical Model		Integrated Model		Hierarchical Model		Integrated Model	
	Average fps	Frame Rate Fluctuation Value	Average fps	Frame Rate Fluctuation Value	Average fps	Frame Rate Fluctuation Value	Average fps	Frame Rate Fluctuation Value
10	120	0.32	120	0.37	120	0.44	120	0.45
100	120	0.39	120	0.45	120	0.47	120	0.44
1000	64.37	0.42	65.47	0.48	64.37	0.53	65.47	0.56
10,000	39.65	0.54	42.43	0.52	39.65	0.66	42.43	0.65
100,000	30.63	0.61	30.74	0.64	29.68	0.69	30.64	0.69

Figure 6. Sequential frames from (**a**–**h**) visualize the horizontal of the large-scale forest scene changes. The camera height is set at 300 m above the terrain, and the camera moved forward from (**a**–**h**).

From the perspective of the frame rate fluctuation value, the smaller the frame rate fluctuation value, the more stable the scene operation [51]. It could be seen that as the number of trees increased, the frame rate fluctuation value also increased. The average frame rate fluctuation value of the scene generated before growth by the hierarchical model was 0.46, the average frame rate fluctuation value of the integrated model was 0.49, and the average frame rate fluctuation value of both after growth was 0.56. In general, the average frame rate fluctuation of the hierarchical model had a relatively small change, and the scene ran more stably than the integrated model's scene.

According to the growth model of the forest hierarchical model, the visual simulation of the growth dynamics in Shanxia Experimental Forest Farm is shown in Figure 7. Figure 7a–e represent the growth status of the forest after 10 years, and Figure 7f–i represent

the growth status of the forest after 20 years. The forest scene we constructed through visualization tools will allow forest managers to conduct logging, selective logging, planting, and other management operations and view the approximate spatial structure of the forest. Combining forest growth simulation with forest grading models changes the visual effect of large-scale forest scenes and improves the usability of forests.
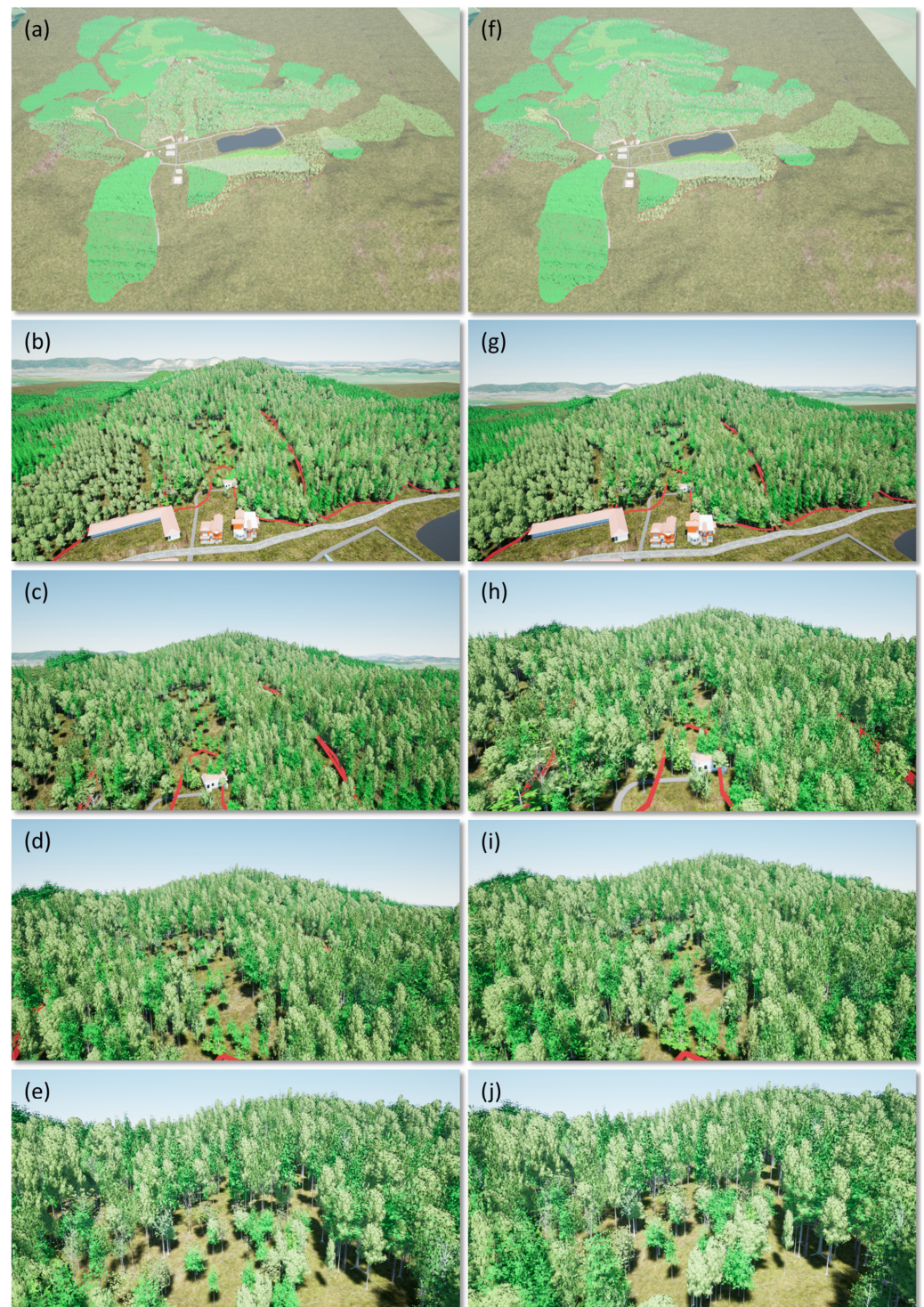

Figure 7. Visual simulation of growth dynamics in Shanxia Forest Farm. (**a**–**e**) Representation of the growth status of the forest after 10 years. (**f**–**j**) Representation of the growth status of the forest after 20 years.

4. Discussion

Visualization is considered one of the most direct ways to explain the results of a forest growth simulation [26,40]. The visualization of large-scale forest scenes serves as a valuable tool for understanding the composition and dynamics of forests. It allows for the representation of natural growth processes and the impacts of disturbances, such as forest harvesting, providing practical guidance for forest management and further research on forest dynamics. However, previous studies have often overlooked the heterogeneity of individual trees in the representation of large-scale forest scenes, resulting in a lack of diversity in the rendered forests. In this study, we proposed a strategy for visualizing large-scale forest scenes by combining a tree hierarchical model with a growth visualization simulation. Using Unreal Engine 4 and LOD (Level of Detail) technology, we constructed initial large-scale forest scenes and simulated forest growth. The results indicated that our proposed method improves the visual landscape of large-scale forest scenes, achieves dynamic growth of large-scale forest scenes, and has good rendering efficiency.

We used the hierarchical model and the integrated model for visual simulation before and after growth. The results showed that the changes in DBH and UBH of the hierarchical model after growth were significant. The integrated model can only reflect the proportion of tree H and DBH, and the UBH, CH, and CW are calculated proportionally on the basis of their size and the calculated H and DBH, which is unreasonable. The crown shape of the hierarchical model is more diverse than the integrated model, which can better explain the community structure characteristics of forests. However, our method does not completely represent the morphological changes in the forest. We improved the issue of tree uniformity and traditional static expression of forest landscapes at the level of large-scale forest landscapes. In addition, we used the forest hierarchical model to construct a large-scale initial forest scene. The average frame rate of the initial forest scene was 30.63 fps. We calculated the growth changes of trees at different ages using the hierarchical model and scaled the hierarchical model according to the values after growth, achieving the dynamic simulation of large-scale forest landscapes. The results showed that the average frame rate of the scene during the growth process of the classification model was 29.68 fps, which met the basic scene rendering requirements. People can intuitively determine the spatial distribution of trees. Furthermore, we invited 20 graduate students to evaluate the simulated scenes by comparing them with real images, resulting in a satisfaction rate of 95%.

This study provides a reasonable and efficient method for constructing diverse and dynamic large-scale forest scenes. By combining Unreal Engine 4 with field survey data on forest inventories, we constructed a three-dimensional model of each tree species and restored a large-scale forest scene of the Shanxia Forest Farm on the basis of the spatial distribution of the tree positions and species composition. In addition, individual trees or stands can be highlighted according to user-defined operations, allowing forest managers to observe the forest at multiple scales, including stands and landscapes. The three-dimensional exploration of the spatial structure of forests and landscapes contributes to evaluating the development and succession of forest ecosystems and optimizes alternative solutions for forest management. This is essential for assessing forest ecosystem development and succession, optimizing forest management alternatives, and promoting a better understanding of natural and human disturbances among managers and researchers. The visualization of dynamic growth in large-scale forest scenes is crucial for evaluating future forest changes and the impacts of forest management measures. However, for large-scale and long-term forest growth simulation, tree mortality may occur. This study lacked an exploration of tree death. In the future, we will consider changes in forest spatial structure caused by factors such as tree death, fire, wind, and logging, and we will conduct a visual simulation, enabling managers and researchers to better understand natural and human interference.

However, accurately simulating forest growth and representing the branching structure of trees remain challenging due to the wide range of growth variation and driving mechanisms involved. Constrained by existing computational resources and power, this

study strikes a balance between frame rate and scene simulation effects by reducing the number of polygons while still capturing the growth status and rendering effects of trees. Our method mainly displays the polymorphism of forests visually. Forest growth does not completely conform to the growth patterns of trees. The system achieves the interpretation and understanding of the output results of the growth model. However, a growth model that is only related to age is too simple. In general, a 4-year-old tree has a smaller crown but also fewer branches, leaves, etc., than a 20-year-old tree. Therefore, we will consider integrating multiple influencing factors, such as stand density, competition index, site index, and environment into the growth model to ensure that the continuous growth of the forest at each stage is in line with reality.

5. Conclusions

In this study, we considered the simplicity and static expression of constructing large-scale forest scenes at present. Using Unreal Engine 4, we utilized three-dimensional visualization simulation technology and LOD technology combined with a forest hierarchical growth model to construct a large-scale forest landscape of 100,000 trees, improving the visual effect of dynamic changes in diverse large-scale forest scenes. The numerical results of tree DBH, height, CW, CH, and UBH were distributed widely before and after growth, which indicated the polymorphism of the forest. However, the integrated model could only be scaled on the basis of the true tree height and DBH. Other factors, such as CW, CH, and UBH, did not conform to the actual growth mode, which was prone to deformation and unreality. In addition, the growth value of the hierarchical growth model calculated by the blueprint function was used to simulate the growth of the forest after 40 and 50 years. The results showed that the average predicted values, average errors, and standard deviations of the UBH and CW of the hierarchical model at 40 and 50 years were smaller than those of the integrated model. The evaluation results of 20 people on the constructed large-scale forest scene showed that the forest scene constructed using this method had a high similarity with the real scene, a strong immersion experience, and a good evaluation rate of 95%. The average frame rate during the initial scene operation was 30.96 fps, the average frame rate during the growth process was 29.68 fps, and the average frame rate fluctuation value of the system operation was 0.46, which ensured the stability of the scene operation. The method proposed in this study for constructing large-scale forest scenes based on hierarchical growth models is applicable to other regions and tree species. It improves the diversity and dynamic change process of large-scale forest scenes visually. In order to analyze the spatial structure characteristics of forests more comprehensively and quantitatively, it is necessary to conduct complex research on growth models for each tree species.

References

1. Franklin, J.F.; Spies, T.A.; Van Pelt, R.; Carey, A.B.; Thornburgh, D.A.; Berg, D.R.; Lindenmayer, D.B.; Harmon, M.E.; Keeton, W.S.; Shaw, D.C.; et al. Disturbances and Structural Development of Natural Forest Ecosystems with Silvicultural Implications, Using Douglas-Fir Forests as an Example. *For. Ecol. Manag.* **2002**, *155*, 399–423. [CrossRef]
2. Hossein, A.; Djamali, M.; Ghorbanalizadeh, A.; And, E.R. Plant Biodiversity of Hyrcanian Relict Forests, N Iran: An Overview of the Flora, Vegetation, Palaeoecology and Conservation. *Pak. J. Bot.* **2010**, *42*, 231–258.

3.   Hof, J.G.; Joyce, L.A. Spatial Optimization for Wildlife and Timber in Managed Forest Ecosystems. *For. Sci.* **1992**, *38*, 489–508. [CrossRef]

4.   Huang, J.; Lucash, M.S.; Scheller, R.M.; Klippel, A. Walking through the Forests of the Future: Using Data-Driven Virtual Reality to Visualize Forests under Climate Change. *Int. J. Geogr. Inf. Sci.* **2021**, *35*, 1155–1178. [CrossRef]

5.   Lange, E. Integration of Computerized Visual Simulation and Visual Assessment in Environmental Planning. *Landsc. Urban Plan.* **1994**, *30*, 99–112. [CrossRef]

6.   Griffon, S.; Coligny, F. de AMAPstudio: A Software Suite for Plants Architecture Modelling. In Proceedings of the 2012 IEEE 4th International Symposium on Plant Growth Modeling, Simulation, Visualization and Applications, Shanghai, China, 31 October–3 November 2012; pp. 141–147.

7.   Li, S.; Zhang, H.; Li, Y.; Yang, T.; Shen, K. Three-Dimensional Visualization Simulation of Chinese Fir Stand Growth Based on Unity3D. In Proceedings of the 2018 3rd International Conference on Mechanical, Control and Computer Engineering (ICMCCE), Huhhot, China, 14–16 September 2018; IEEE: Piscataway, NJ, USA, 2018; pp. 530–534.

8.   Schroeder, W.J.; Zarge, J.A.; Lorensen, W.E. Decimation of Triangle Meshes. In Proceedings of the 19th Annual Conference on Computer Graphics and Interactive Techniques, Chicago, IL, USA, 27–31 July 1992; pp. 65–70.

9.   Kalvin, A.D.; Taylor, R.H. Superfaces: Polygonal Mesh Simplification with Bounded Error. *IEEE Comput. Graph. Appl.* **1996**, *16*, 64–77. [CrossRef]

10.   Lluch, J.; Camahort, E.; Vivó, R. An Image-Based Multiresolution Model for Interactive Foliage Rendering. *J. WSCG* **2004**, *12*, 507–514.

11.   Max, N. Optical Models for Direct Volume Rendering. *IEEE Trans. Vis. Comput. Graph.* **1995**, *1*, 99–108. [CrossRef]

12.   Feng, W.; Gang, W.; Deji, P.; Yuan, L.; Liuzhong, Y.; Hongbo, W. A Parallel Algorithm for Viewshed Analysis in Three-Dimensional Digital Earth. *Comput. Geosci.* **2015**, *75*, 57–65. [CrossRef]

13.   Weber, J.; Penn, J. Creation and Rendering of Realistic Trees. In Proceedings of the 22nd Annual Conference on Computer Graphics and Interactive Techniques, Los Angeles, CA, USA, 6–11 August 1995; pp. 119–128.

14.   Remolar, I.; Chover, M.; Belmonte, O.; Ribelles, J.; Rebollo, C. Geometric Simplification of Foliage. In Proceedings of the Eurographics (Short Presentations), Saarbrücken, Germany, 2–6 September 2002.

15.   Lluch, J.; Vicent, M.J.; Fernandez, S.; Monserrat, C.; Vivo, R. The Modelling of Branched Structures Using a Single Polygonal Mesh. In Proceedings of the VIIP, Marbella, Spain, 3–5 September 2001; pp. 203–207.

16.   Perbet, F.; Cani, M.-P. Animating Prairies in Real-Time. In Proceedings of the 2001 Symposium on Interactive 3D Graphics, Chapel Hill, NC, USA, 26–29 March 2001; pp. 103–110.

17.   Marshall, D.; Fussell, D.S.; Campbell III, A.T. Multiresolution Rendering of Complex Botanical Scenes. In Proceedings of the Graphics Interface, Kelowna, BC, Canada, 21–23 May 1997; Volume 97, pp. 97–104.

18.   Meyer, A.; Neyret, F.; Poulin, P. Interactive Rendering of Trees with Shading and Shadows. In Proceedings of the Rendering Techniques 2001: Proceedings of the Eurographics Workshop, London, UK, 25–27 June 2001; Springer: Berlin/Heidelberg, Germany, 2001; pp. 183–196.

19.   Lim, E.-M.; Honjo, T. Three-Dimensional Visualization Forest of Landscapes by VRML. *Landsc. Urban Plan.* **2003**, *63*, 175–186. [CrossRef]

20.   Decaudin, P.; Neyret, F. Rendering Forest Scenes in Real-Time. In Proceedings of the EGSR04: 15th Eurographics Symposium on Rendering, Norrköping, Sweden, 21–23 June 2004; pp. 93–102.

21.   Larsen, D.R.; Scott, I. The Sylview Graphical Interface to the SYLVAN STAND STRUCTURE Model with Examples from Southern Bottomland Hardwood Forests. In Proceedings of the 14th Biennial Southern Silvicultural Research Conference, Gen Tech. Rep SRS-121, Asheville, NC, USA, 1 January 2010; Department of Agriculture, Forest Service, Southern Research Station: Asheville, NC, USA, 2010.

22.   Li, Z.; Zhang, Y.-D. 3D Reconstruction Method of Forest Landscape Based on Virtual Reality. *Multimed. Tools Appl.* **2020**, *79*, 16369–16383. [CrossRef]

23.   Tianyang, D.; Jiajia, X.; Jing, F.; Ling, Z. Fast Generation of Large-Scale Forest Scene Based on Spatial Similarity. *Int. J. Digit. Content Technol. Appl.* **2012**, *6*, 13.

24.   Schaufler, G.; Stürzlinger, W. A Three Dimensional Image Cache for Virtual Reality. *Comput. Graph. Forum* **1996**, *15*, 227–236. [CrossRef]

25.   Bai, Z.Y.; Huang, X.Y. Plum Tree Visualization Based on Speed Tree. *Key Eng. Mater.* **2011**, *474*, 511–516. [CrossRef]

26.   Li, S.; Zhang, H.; Li, Y.; Yang, T.; He, J.; Ma, Z.; Shen, K. Dynamic Visual Simulation of Chinese Fir Stand Growth Based on Sample Library. *For. Res.* **2019**, *32*, 21–30. (In Chinese)

27.   Li, Y.; He, J.; Yu, S.; Wang, H.; Ye, S. Spatial Structures of Different-Sized Tree Species in a Secondary Forest in the Early Succession Stage. *Eur. J. For. Res.* **2020**, *139*, 709–719. [CrossRef]

28.   Tang, L.; Peng, X.; Chen, C.; Huang, H.; Lin, D. Three-Dimensional Forest Growth Simulation in Virtual Geographic Environments. *Earth Sci. Inform.* **2019**, *12*, 31–41. [CrossRef]

29.   Zamuda, A.; Brest, J. Vectorized Procedural Models for Animated Trees Reconstruction Using Differential Evolution. *Inf. Sci. (NY)* **2014**, *278*, 1–21. [CrossRef]

30.   Tang, L.; Chen, C.; Huang, H.; Lin, D. An Integrated System for 3D Tree Modeling and Growth Simulation. *Environ. Earth Sci.* **2015**, *74*, 7015–7028. [CrossRef]

31.   Ijiri, T.; Owada, S.; Igarashi, T. The Sketch L-System: Global Control of Tree Modeling Using Free-Form Strokes. In Proceedings of the Smart Graphics: 6th International Symposium, SG 2006, Vancouver, BC, Canada, 23–25 July 2006; Proceedings 6. Springer: Berlin/Heidelberg, Germany, 2006; pp. 138–146.
32.   Peng, W.; Pukkala, T.; Jin, X.; Li, F. Optimal Management of Larch (Larix Olgensis A. Henry) Plantations in Northeast China When Timber Production and Carbon Stock Are Considered. *Ann. For. Sci.* **2018**, *75*, 63. [CrossRef]
33.   Xie, L.; Widagdo, F.R.A.; Dong, L.; Li, F. Modeling Height–Diameter Relationships for Mixed-Species Plantations of Fraxinus mandshurica Rupr. and Larix olgensis Henry in Northeastern China. *Forests* **2020**, *11*, 610. [CrossRef]
34.   Miina, J.; Pukkala, T. Using numerical optimization for specifying individual-tree competition models. *For. Sci.* **2000**, *46*, 277–283.
35.   Dong, L.; Pukkala, T.; Li, F.; Jin, X. Developing Distance-Dependent Growth Models from Irregularly Measured Sample Plot Data—A Case for Larix Olgensis in Northeast China. *For. Ecol. Manag.* **2021**, *486*, 118965. [CrossRef]
36.   Pukkala, T. Methods to Describe the Competition Process in a Tree Stand. *Scand. J. For. Res.* **1989**, *4*, 187–202. [CrossRef]
37.   Packalen, P.; Pukkala, T.; Pascual, A. Combining Spatial and Economic Criteria in Tree-Level Harvest Planning. *For. Ecosyst.* **2020**, *7*, 18. [CrossRef]
38.   Anastacio, F.; Prusinkiewicz, P.; Sousa, M.C. Sketch-Based Parameterization of L-Systems Using Illustration-Inspired Construction Lines and Depth Modulation. *Comput. Graph.* **2009**, *33*, 440–451. [CrossRef]
39.   Letort, V.; Cournède, P.-H.; Mathieu, A.; De Reffye, P.; Constant, T. Parametric Identification of a Functional–structural Tree Growth Model and Application to Beech Trees (Fagus sylvatica). *Funct. Plant Biol.* **2008**, *35*, 951–963. [CrossRef]
40.   Bailey, R.L.; Dell, T.R. Quantifying Diameter Distributions with the Weibull Function. *For. Sci.* **1973**, *19*, 97–104.
41.   Bailey, R.L.; Cieszewski, C.J. Development of a Well-Behaved Site-Index Equation: Jack Pine in North-Cental Ontario: Comment. *Can. J. For. Res.* **2000**, *30*, 1667. [CrossRef]
42.   Feng, L.; De Reffye, P.; Dreyfus, P.; Auclair, D. Connecting an Architectural Plant Model to a Forest Stand Dynamics Model—Application to Austrian Black Pine Stand Visualization. *Ann. For. Sci.* **2012**, *69*, 245–255. [CrossRef]
43.   De Reffye, P.; Edelin, C.; Françon, J.; Jaeger, M.; Puech, C. Plant Models Faithful to Botanical Structure and Development. *ACM Siggraph Comput. Graph.* **1988**, *22*, 151–158. [CrossRef]
44.   Akarsu, E.; Fox, G.; Haupt, T.; Kalinichenko, A.; Kim, K.-S.; Sheethaalnath, P.; Youn, C.-H. Using Gateway System to Provide a Desktop Access to High Performance Computational Resources. In Proceedings of the Eighth International Symposium on High Performance Distributed Computing (Cat. No. 99TH8469), Redondo Beach, CA, USA, 6 August 1999; IEEE: Piscataway, NJ, USA, 1999; pp. 294–298.
45.   Castel, T.; Caraglio, Y.; Beaudoin, A.; Borne, F. Using SIR-C SAR Data and the AMAP Model for Forest Attributes Retrieval and 3-D Stand Simulation. *Remote Sens. Environ.* **2001**, *75*, 279–290. [CrossRef]
46.   Madureira, L.; Nunes, L.C.; Borges, J.G.; Falcão, A.O. Assessing Forest Management Strategies Using a Contingent Valuation Approach and Advanced Visualisation Techniques: A Portuguese Case Study. *J. For. Econ.* **2011**, *17*, 399–414. [CrossRef]
47.   Meng, X.Y. *Forest Mensuration*; Chinese Forestry Publishing House: Beijing, China, 2006.
48.   Luo, J.; Dai, C.; Tian, Y.; Peng, P.; Ma, F.; Zeng, Z.; Zhou, X.; Zhang, M. The tree height and DBH growth model of establishment of main constructive species for Project Forests of Carbon Sink in Hunan Province. *Hunan For. Sci. Technol.* **2016**, *43*, 46–50. (In Chinese)
49.   Ma, Z.; Zhang, H.; Li, Y.; Yang, T.; Chen, Z.; Li, S. Visual Simulation of Chinese Fir Crown Growth Based on Spatial Structure. *For. Res.* **2018**, *31*, 150–157. (In Chinese)
50.   Lei, K.; Zhang, H.; Qiu, H.; Liu, Y.; Hu, X.; Wang, J.; Cui, Z.; Zuo, Y. Comprehensive Decision Index of Logging (CDIL) and Visual Simulation Based on Horizontal and Vertical Structure Parameters. *Forests* **2023**, *14*, 277. [CrossRef]
51.   Garg, K.; Nayar, S. Photorealistic Rendering of Rain Streaks. *ACM Trans. Graph.* **2006**, *25*, 996–1002. [CrossRef]